Natural-based chiral task-specific deep eutectic solvents: a novel, effective tool for enantiodiscrimination in electroanalysis

Serena Arnaboldi[a§], Andrea Mezzetta[b§], Sara Grecchi[a], Mariangela Longhi[a], Elisa Emanuele[a], Simona Rizzo[c], Fabiana Arduini[d], Laura Micheli [d], Lorenzo Guazzelli[b*], Patrizia Romana Mussini[a*]

a. *Dipartimento di Chimica, Università degli Studi di Milano, Via Golgi 19, 20133 Milano (Italia).*
E-mail: patrizia.mussini@unimi.it
b. *Dipartimento di Farmacia, Università degli Studi di Pisa, Via Bonanno 33, 56126 Pisa (Italia).*
E-mail: lorenzo.guazzelli@unipi.it
c. *CNR Istituto di Scienze e Tecnologie Chimiche "Giulio Natta", Via C. Golgi 19, 20133 Milano (Italia).*
d. *Dipartimento di Scienze e Tecnologie Chimiche, Università degli Studi di Roma Tor Vergata, Via della Ricerca Scientifica, 1 00133 Roma (Italia)*

§ Co-first authors
**Co-corresponding and co-last authors.*

Abstract

Deep Eutectic Solvents (DESs) offer advantages similar to ionic liquid (IL) ones, with easier and more sustainable synthesis; moreover, bio-based DESs often include chiral components, surprisingly underexploited. A proof of concept is now offered of the impressive potential of enantiopure chiral DESs as chiral media for enantioselective electroanalysis. Three chiral DESs, consisting of a molecular salt with bio-based chiral cation $[NopolMIm]^+$ combined with three natural and/or low-cost partners (levulinic acid, glycerol and urea), are introduced and investigated as chiral voltammetry media. Significant potential differences are observed for the enantiomers of a model chiral probe, with a dramatic tuning depending on the achiral DES component, reaching an impressive ~0.5 V in the levulinic acid case (while less efficient appears $[NopolMIm]^+$ as chiral additive in IL). With the same medium good enantiodiscrimination is also observed for aminoacid tryptophan, a quite different probe and of applicative interest. These findings can be considered as a remarkable step further in chiral electroanalysis as well as in the development of task-specific enantioselective media.

Keywords: Chiral Bio-Based Deep Eutectic Solvents • Chiral Electroanalysis• Enantiodiscrimination of electroactive probe enantiomers • Chiral voltammetry on SPEs • Task-specific enantioselective media

Introduction

Deep eutectic solvents (DESs) are rapidly growing in popularity as attractive media for a variety of applications [1-4]. This interest follows from their featuring many advantageous properties similar to ionic liquids (ILs), combined with lower cost and easier preparation as well as, possibly, higher biocompatibility and biodegradability [1,2,4] particularly if made of biobased components (natural deep eutectic solvents, NADES) [5-7].

A further DES advantage is their exceptionally wide and easy modulability in composition and properties, which is implicit in their definition. Unlike ILs, DESs are not pure compounds constituted by anions and cations alone, but mixtures of Lewis or Brønsted acids and bases, like for instance a hydrogen bond acceptor HBA (often a quaternary N salt) and a hydrogen bond donor HBD (often an alcohol, polyol, carboxylic acid, amine, carbohydrate, or urea), that have an eutectic point at a temperature quite below the one predicted for an ideal mixture [8]. It is worthwhile noticing that single DES components could have more than one binding site, even of different character, resulting in more complex interactions between the two partners; as a result, it may be more appropriate to describe them in terms of prevailing hydrogen bond donor or acceptor character. In any case, according to the above definition, to assess the real DES nature of a new mixture requires to obtain its experimental phase diagram, to be compared to the ideal predicted one. Importantly, although the non-ideal lowering of the eutectic melting point is linked to strong specific interactions between the eutectic components, the eutectic composition may not correspond to a stoichiometric 1 : n proportion between the component mole fractions, since it results from a combination of ideal fusion properties and 1 : n specific interactions between the mixture components [8]. On the other hand, it is not required for the operating mixture to have the exact composition of the eutectic point to be considered a DES, but any component mixture in the liquid state at a working temperature below the ideal eutectic point can be considered as a DES. This allows for modulation of DES properties by changing the component ratio [8].

In analogy to ILs, DESs look particularly attractive as electrochemistry and electroanalysis media, on account of peculiar transport and solvation properties as well as convenient potential windows [3], with redox active molecules featuring reasonable diffusion coefficients, nearly unaffected by charges [9] and electron transfer (ET) rate constants considerably higher respect to the IL case.[10] Accordingly, an increasing number of electrochemical applications have recently appeared, particularly concerning electrodepositions and sensing [3], like for ILs.

A frontier application worthy to be explored is represented by enantioselective electrochemistry and electroanalysis, particularly in terms of obtaining significant potential differences for the antipodes of electroactive probes, in order to easily discriminate them (with possible concurrent quantification from current evaluation) or selectively activate the desired one [11]. This of course requires the enantiomers to undergo electron transfer (ET) processes in energetically different conditions, which can be achieved implementing suitable enantiopure chiral selectors at the interphase, either at the electrode surface or in the medium, resulting in diastereomeric ET contexts for the two enantiomers [11]. Most approaches have so far focused on the first strategy, *i.e.* the chiral electrode one [11], while comparatively less have been those based on achiral electrodes in media implemented with chirality (*e.g.* in the solvent, or supporting electrolyte, or in additives/ complexing agents/ mediators...) [11]. However, a breakthrough can be achieved with chirality implemented in highly ordered media, like ILs, which imply electrochemical processes to take place at an interphase of very high intrinsic order [12-17], resembling bulk liquid crystal features at least close to the charged electrode surface. Such high structural order has been recently experimentally demonstrated to extend for many layers up to a considerable distance from the surface [16], with significant modulation according to the IL ion combination [17] and to the possible presence of coadsorbed species, including water (with the IL character holding up to considerable amounts of the latter) [18,19]. Actually significant differences in voltammetry peak potentials [11,16-24] have been recently

observed for the enantiomers of chiral probes working on achiral electrodes in commercial achiral ILs with the addition of small amounts of chiral molecular salts, either solid at room temperature or liquid (and therefore chiral ionic liquids CILs), or in bulk CILs. Such attractive results, particularly impressive in the case of salts with "inherently chiral" cations of axial or helical stereogenicity [20,21,24] (with potential differences of even hundreds of mVs for probe enantiomers, in analogy with the powerful performances of electrode surfaces modified with inherently chiral films, *e.g.* [25]), have been justified considering the highly ordered interphase between the charged electrode and the ionic liquid medium, the latter containing chiral cations either in massive amount (bulk CIL) or even moderate (IL with chiral salt additives). In the latter case, a local "chiral mouldering" effect could be assumed, by analogy with nematic to cholesteric phase transitions induced by chiral additives in bulk liquid crystals [20, 26-28] or "liquid crystalline ionic liquids" [29,30]. Moreover, the semisolid, highly structured context at the charged interphase could also locally promote or enhance specific interactions between probe and selector.

In this context, it is important to investigate whether DESs, sharing so many attractive properties with ILs, would also prove effective for this extremely advanced application, possibly with the additional advantage of easier and less expensive availability. In fact, attractively, the DES definition implies that chiral DESs can be prepared by choosing at least one chiral donor or acceptor component, either from the natural pool or synthetic ones, and many DES based on natural components are actually chiral and even enantiopure [5-7]. However, in most cases such components are chosen and exploited on account of their natural origin, low cost as well as "scalar" physicochemical properties, not on account of their chirality. Surprisingly, only very few examples have so far been described of intentional exploitation of the chiral properties of DES components. These include a series of monosaccharide-based DES for the development of CPL emitting materials, based on HBD derived from biomass, glucose, and fructose [31] and a series of DES consisting of a chiral HBD (camphorsulphonic acid) and a chiral HBA, *N,N,N*-trimethyl-(1-phenylethyl)ammonium methanesulfonate (in this report, focus is on the effect of the combination of both DES component configurations on the enantiomeric excess obtained in a model Friedel-Crafts Michael-type addition [32]).

To our knowledge, the application of chiral DESs as media to achieve enantioselective electroanalysis and electrochemistry has not been documented yet. Clearly, considering the above very successful IL cases, a key issue concerns the degree and kind of structural order of DESs at the interphase with a charged electrode. Unfortunately, unlike the IL case, only a few first studies are so far available [33-41]. Indeed the subject is very complex to treat respect to the IL case [37]. However, considering for instance the very popular cases of DESs consisting of a quaternary N salt HBA in 1:2-1:4 molar ratio with an alcohol, polyol, carboxylic acid, amine, carbohydrate, or urea as HBD, they could be expected to have intermediate features between the limiting cases of

i) ILs, entirely consisting of ions, including at least one with long alkyl chains; their structure is mainly based on strong coulombic interactions between net charges, with some contribution from van der Waals interactions increasing with increasing alkyl chain length; at the charged electrode they display a very strong and regular order, consisting of many ionic layers, like a semisolid crystal [12-19];

ii) classical (solvent + supporting electrolyte) electrochemistry media, which imply solvent-solvent interactions based on hydrogen bonding and/or van der Waals interactions, plus ion-dipole and ion-ion interactions concerning ionic species typically present in small amount (2-4 w% for ~0.1 M supporting electrolytes); the charged electrode surface is faced by a layer of ions of opposite charge from the supporting electrolyte (in the absence of specific adsorption, on the "outer Helmholtz plane" after a layer of solvent dipolar molecules) but respect to the IL case the charged surface polarization effects are lost at very short distance.

Actually the first studies point to a local DES order consisting of multiple layers [33-35,39,40]; such interphase structure, strongly influenced by the electrode potential determining the surface charge

[29,33] and by the cation alkyl chain length [36], looks by far less tight respect to the IL case, with the molecular component favouring packing over layering [33] with alkyl chains tending to associate into clusters [34]; moreover, it fades within just a few nm from the electrode surface [33,34,39]. Surprisingly, however, such DES interphase structure holds up to 30-50 wt% of water, with water even incorporated/cooperating in the structural order [38,39] (the same also holds for bulk DES order, although within a lower reported threshold of 0.4/0.5 mole fraction water, corresponding to several wt% only [42]); this is a great advantage for electrochemical applications, enabling to simplify the operating conditions and to widely modulate the medium properties [40,42] (for example, to lower resistance and viscosity) while maintaining DES interphacial properties [38,39].
At the same time, as above mentioned, DESs look advantageously closer to molecular solvents respect to ILs in terms of electron transfer rate constants [10] as well as diffusion coefficient features [9].
Thus overall DESs apparently display specifical advantages over ILs for electrochemistry experiments while maintaining a certain degree of peculiar local order. It is therefore quite attractive to investigate whether in the case of a chiral DES such local order, although less defined and expanded than the IL one, can still be sufficient for effective enantiodiscrimination in electron transfers involving chiral electroactive probes.
We recently introduced a new family of chiral biobased salts, a selection of which were also tested as CILs and/or CIL additives in bulk ILs for voltammetry enantiodiscrimination experiments, with promising features that could be assumed to apply to the whole family [22]. The salt family includes 3-{2-[(1R,5S)-6,6-dimethylbicyclo[3.1.1]hept-2-enyl]ethyl}-1-methyl-1H-imidazol-3-ium methanesulfonate ([NopolMIm] Mes, precursor of the corresponding bistriflimide CIL [22], Figure 1), which appears to be a good candidate as DES component in conjunction with appropriate HBD partners on account of its methanesulfonate anion of strong HBA character. Other family members with bistriflimide anions look less convenient not only because of the additional required metathesis step and of their being expensive and environmentally unfriendly, but also because of their lower HBA character compared with methanesulfonate homologues.

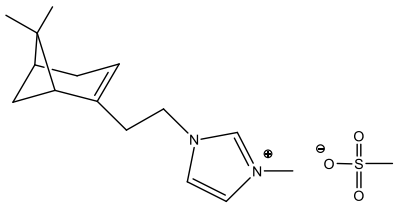

Figure 1. The DES chiral bio-based component [NopolMIm] Mes (3-{2-[(1R,5S)-6,6-dimethylbicyclo-[3.1.1]hept-2-enyl]ethyl}-1-methyl-1H-imidazol-3-ium methanesulfonate) [22]

Counteranion methanesulfonate is also quite preferable from the electrochemical perspective with respect to halide ones, which are often featured in DES [43], because halide anions are quite electrochemically active, resulting in a much narrower potential window on the oxidation side as well as in specific adsorption phenomena in suitable conditions.
Thus an original series of electroanalytical enantiodiscrimination experiments is now presented, performed with model electroactive chiral probes in three chiral DESs prepared combining chiral [NopolMIm] Mes with convenient HBA partners, aiming to achieve a sound proof-of-concept of the remarkable potentialities of chiral DESs for enantioselective electroanalysis. Moreover, for comparison's sake, the same protocol is also investigated using the same chiral selector as 0.05 M additive in achiral IL BMIMTf$_2$N.

Results and DIscussion

Chiral [NopolMIm] Mes [22] was combined with three natural and/or low-cost HBDs, often employed in the preparation of DESs, including

- a weak ketoacid, levulinic acid (4-oxopentanoic acid);
- a polyalcohol, glycerol;
- a NH donor, urea.

The DES character of the three resulting binary systems was evaluated by differential scanning calorimetry (DSC), comparing experimental temperature data for melting (or solid/liquid glass transition) with "ideal" phase diagrams, calculated assuming no specific interactions between components in the liquid phase [8,43]. Such diagrams (solid lines in Figure 2) were obtained in terms of melting T *vs* x_i curves for the binary mixture components A and B, their intersection providing the eutectic point. Such curves were calculated from the thermodynamic equations accounting for the activity in the liquid phase of the binary mixture components A and B as a function of temperature [8],

$$\ln(x_A\gamma_A) = \left(\frac{\Delta H_{m,A}}{R}\right)\left(\frac{1}{T_{m,A}}-\frac{1}{T}\right) + \left(\frac{\Delta C_{p,m,A}}{R}\right)\left(\frac{T_{m,A}}{T} - \ln\left(\frac{T_{m,A}}{T}\right) - 1\right) \quad (1)$$

$$\ln(x_B\gamma_B) = \left(\frac{\Delta H_{m,B}}{R}\right)\left(\frac{1}{T_{m,B}}-\frac{1}{T}\right) + \left(\frac{\Delta C_{p,m,B}}{R}\right)\left(\frac{T_{m,B}}{T} - \ln\left(\frac{T_{m,B}}{T}\right) - 1\right) \quad (2)$$

assuming γ_A, γ_B =1 as in ideal liquid mixture [44], and employing experimental data of melting temperatures $T_{m,A}$ and $T_{m,B}$, molar melting enthalpies $\Delta H_{m,A}$ and $\Delta H_{m,B}$, and variations of molar heat capacities from the solid to the liquid state $\Delta C_{p,m,A}$ and $\Delta C_{p,m,B}$, for the two pure components A and B.

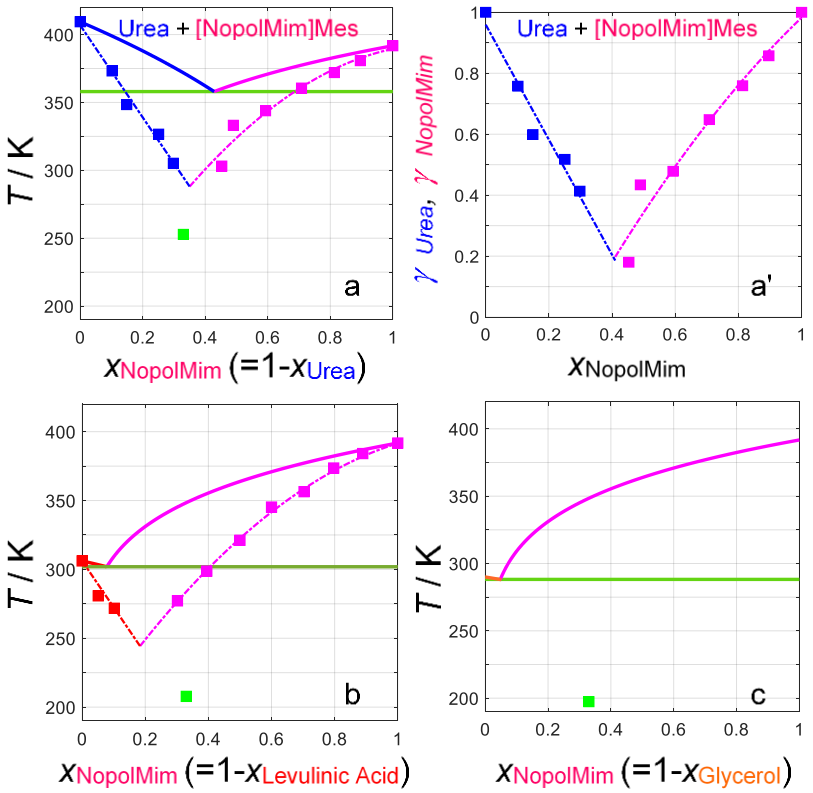

Figure 2. Estimated "ideal" eutectic diagrams (solid lines) and experimental onset temperatures for melting (blue and pink squares) or glass transitions (green squares) at different system compositions. For DES U also experimental activity coefficients are provided.

Comparing the three cases in order of decreasing melting temperature of the HBD component, that is, urea (T_m ~136 °C, Figure 2a), levulinic acid (T_m~33°C, Figure 2b) and glycerol (T_m~17 °C, Figure 2c), the "ideal" eutectic mole fraction in the chiral HBA component [NopolMIm] Mes (having T_m ~119 °C; a detailed DSC study is reported at SI 1) remarkably decreases from slightly above 0.4 to very low values (~0.1 and ~0.05), as for rather low molar ratios of the HBA salt in the HBD component. At the same time the "ideal" eutectic temperature decreases from significantly above room temperature

(~75 °C) to just above room temperature (~30 °C), to slightly below room temperature (~10 °C); in the last two cases the melting point lowering respect to the pure HBD component is very small. However, quite different are the trends of the experimental onset temperatures for melting, obtained across the whole composition range of the binary systems with HBD urea and levulinic acid. They are reported in Figures 2a and 2b as squares, interpolated by dash-and-dot lines; the latter ones should converge in the eutectic melting point; however, it should only be considered a virtual one, since, in agreement with literature cases [45,46], close to the eutectic composition only glass transitions, located quite below the above extrapolated melting point, are observed, rather than melting points possibly followed by glass transitions.

Thus, real phase equilibria show strong deviations respect to the corresponding ideal ones (also highlighted in terms of dramatic decrease of the activity coefficients calculated from the above equations with experimental *x*/*T* data, Figure 2a'). In particular:

(*i*) in both cases a shift is observed in the eutectic point composition, particularly remarkable in the levulinic acid case, towards a higher content of the higher melting component (urea in the first case, [NopolMIm]Mes in the second case);

(*ii*) at the same time, a dramatic lowering is observed for the melting temperatures respect to ideal ones on both converging curves, pointing to a huge decrease of the eutectic temperature. Thus, for both binary systems, the DES requirement of having a eutectic point at a temperature quite below the one predicted for an ideal mixture, is surely satisfied. Moreover, as mentioned above, any component mixture in the liquid state at a working temperature below the ideal eutectic point can be considered as a DES. In this perspective, a large interval of DES media looks available in both cases, although the composition range shrinks, especially in the urea case, if we only consider temperatures below 25 °C and aim to use the mixtures as liquid media at room temperature.

A good choice in both cases looks selecting $x_{[NopolMIm]Mes}$ ~0.33, implying a 1:2 [NopolMIm]Mes: HBD partner ratio; the resulting media will be hence referred as DES A in the case of levulinic acid and DES U in the case of urea. The same composition was also adopted for the case of glycerol, verifying that the corresponding mixture (DES G) has a much lower glass transition point than the theoretical eutectic temperature (Figure 2c), and therefore can be considered as a DES, too. DSC curves for [NopolMIm]Mes and for DES A, DES U and DES G are reported in SI 2.a and 2.b respectively.

The electrochemical windows of bulk DES A and DES G (DES U, the highest melting DES in the series, is very viscous and requires addition of a small water quantity to be applied for electrochemical experiments at room temperature, a quite acceptable modulation according to the above cited literature [39,40], resulting all the same in a DES interphase) were explored with cyclic voltammetry in thin layers on screen printed electrode cells with graphite working electrodes and $Ag|Ag^+$ pseudoreference electrodes. As shown in Figure 3, the new chiral media have convenient potential windows for electrochemical experiments, about 3 V wide, with reasonable extension on both the oxidation and reduction side.

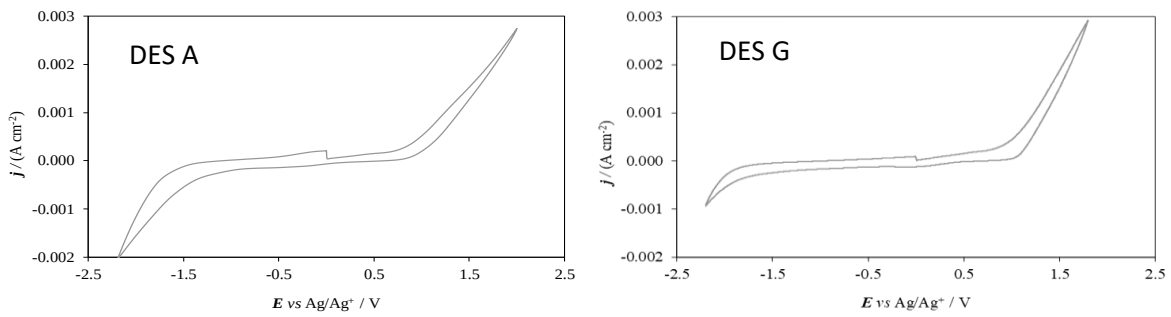

Figure 3. CV potential windows (at 0.2 V/s scan rate) of bulk DES A and DES G, as thin films spread on screen printed electrode cells with graphite working and counter electrodes and $Ag|Ag^+$ pseudoreference electrodes.

The same two DESs were also studied by electrochemical impedance spectroscopy EIS as thin films on a flat cell with concentric graphite electrodes. The recorded EIS features (Figure 4) are numerically well fitted by a $(RC)Q_1Q_2$ equivalent circuit, with R and C accounting for the bulk electrolyte resistance and capacitance (dominating at high frequencies, with $\tau_{RC} = RC$) and constant phase elements Q_i, associated to reactance $Z_{Qi} = 1/(i\omega M_i^{ni})$, dominating at medium low (Q_1) and low (Q_2) frequencies. Numerical fitting of experimental data gives values for all the above parameters (details in SI.3), including

(*i*) $n_1 = 0.40/0.41$, *i.e.* approaching the 0.5 value typical of a Warburg element accounting for diffusive control; actually, considering the nice rationalization provided in [47], this frequency domain should account for ion diffusion (with $\tau_D = L^2/D$) limiting the charging process;

(*ii*) $n_2 = 0.98/1.0$, *i.e.* approaching the ideal capacitance behaviour, clearly accounting for the double layer capacitance at the two interphases.

The electrolyte resistance R is also perceivable as semicircle diameter in the Nyquist diagram (4a) and as horizontal plateau in the Bode modulus plot (4b). Specific conductance (or conductivity) κ can be estimated from $R = 1/\kappa \cdot$ cell constant (cm^{-1}) by comparison with 0.1 *m* KCl (a IUPAC standard [48]), resulting in the 0.1–0.3 mS/cm range, significantly lower than that of bulk ionic liquid 1-butyl-3-methylimidazolium bis(trifluoromethylsulfonyl)imide $BMIMTf_2N$, as such or with 0.05 M [NopolMIm]Mes as chiral additive, but still acceptable for electrochemical experiments.

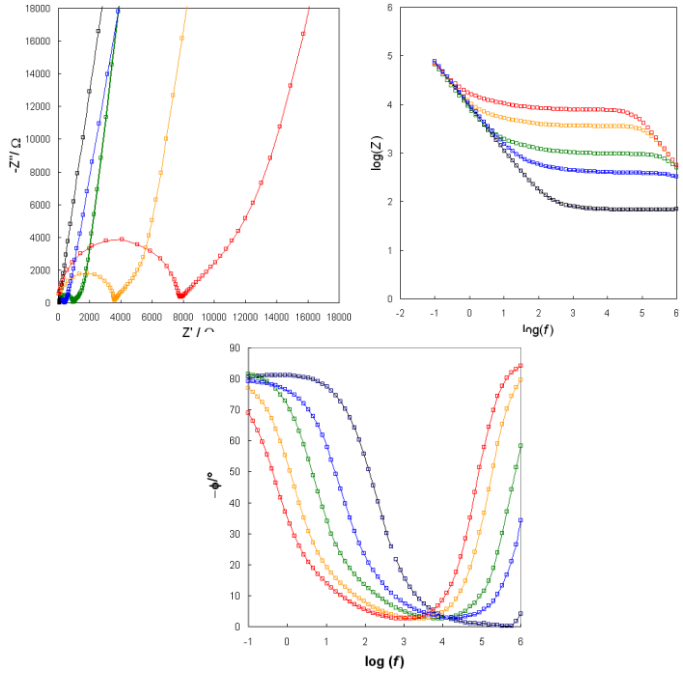

Figure 4. EIS features (as Nyquist, Bode modulus and Bode phase diagrams) of DES A and DES G (red and orange, respectively) as films on a flat conductivity cell with concentric graphite electrodes. The features are also reported of standard 0.1 *m* KCl (black) and of ionic liquid $BMIMTf_2N$, as such (blue) and with 0.05 M [NopolMIm]Mes as chiral additive (green)

The three chiral DESs, DES A, DES G and DES U, were tested as selector media in voltammetry enantiodiscrimination experiments, to our knowledge the first example so far of such an application. The study also included ionic liquid $BMIMTf_2N$ with 0.05 M [NopolMIm]Mes as chiral additive, for comparison's sake.

Comparative voltammetry tests in the above media were performed with enantiomer probes (*R*)-(+)- or (*S*)-(–)-*N,N'*-dimethyl-1-ferrocenylethylamine (henceforth labelled (*R*)-Fc and (*S*)-Fc), our usual choice as model probes when testing chiral electrode surfaces and media, due to their chemical and electrochemical reversibility as well as commercial availability. It is also interesting to note that in

the present case such probes, including a tertiary amino group as one of the stereocentre substituents, can have acid/base interactions with the levulinic acid component in DES A.
(*R*)-Fc and (*S*)-Fc were studied by differential pulse voltammetry DPV, both alone and in mixtures, in small solution volumes at concentrations in the 0.05-0.0075 M range, on screen-printed electrode SPE cells. In all cases a small volume of aqueous KCl solution (0.003 cm^3 per 0.1 cm^3 DES A and DES G, 0.006 cm^3 per 0.1 cm^3 in the case of more viscous DES U) was added to the chiral medium, to stabilize the potential of the pseudoreference electrode, besides advantageously resulting in lower viscosity (an important issue, especially in the DES U case); again, such addition should be regarded as fully compatible with a DES-like interphase considering the above cited literature [39,40]. Three models of SPE cells were considered, one with graphite working electrodes and two with gold working electrodes (details in SI), verifying that enantiodiscrimination could be achieved on all of them, although gold electrodes resulted in better performances. A synopsis of DPV features of single (*R*)-Fc and (*S*)-Fc solutions in the four tested media on Au SPE is reported in Figure 5.

Figure 5. A synopsis of DPV features of (*R*)-Fc and (*S*)-Fc solutions on Au SPE in different chiral media based on

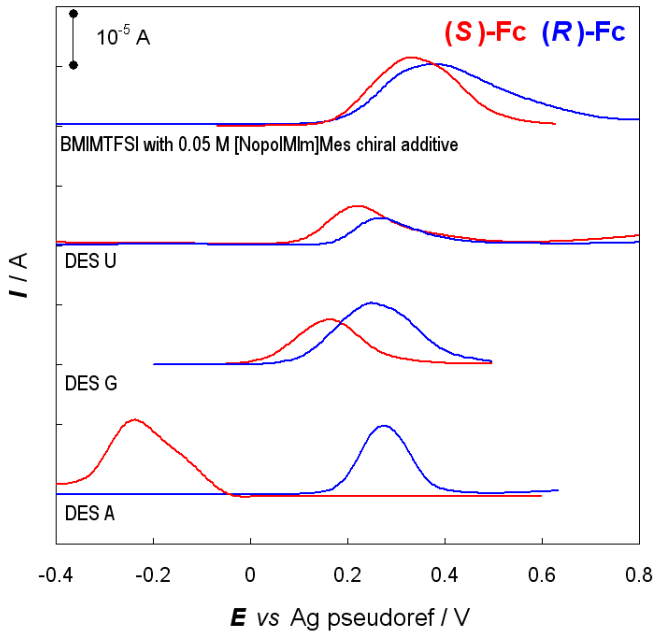

[NopolMIm]Mes as chiral selector.

Enantiodiscrimination in terms of significant potential differences is observed in all cases.
This important feature can be justified in terms of significantly different energy conditions for the electron transfer for the two enantiomers, resulting from diastereoisomeric interactions with the enantiopure environment, which could rely:

- on one hand, on a (supramolecular) peculiar chiral DES order at the interphase at the charged electrode, probably less tight than in the ILs case, and with stronger contribution of packing/clustering respect to ion layering effects, but still effective at least close to the electrode surface, according to the above discussed literature [33-40];
- on the other hand, on (molecular) specific interactions between chiral DES cations and chiral probe molecules; in fact, even mild coordination (here supported *e.g.* by the presence of heteroatoms and aromatic systems) is known to result in significant potential shift for an electroactive probe undergoing electrochemically reversible electron transfer. In particular [49], the potential is known to shift by $(k/n)\log K$ (*i.e.*, considering a one-electron process, by about 60 mV per decade in coordination constant K) plus an additional $(k/n)\log c_L$ contribution linked to the ligand concentration; the shift direction depends on coordination stabilizing the electron transfer reactant or product.

Of course, both the above effects should increase with increasing concentration of the chiral selector component in the medium, and, indeed, the selector concentration has been pointed to as an important factor, resulting in a regular increase of the enantiomer peak potential difference in the case of bipyridine-based inherently chiral additives in achiral ionic liquids [20]. In the case of the family of biobased chiral molecular salts which includes [NopolMIm]Mes, tests on salts liquid at room temperature consisting of cations very similar to $[NopolMIm]^+$ in combination with anion bistriflimide, only showed limited improvements when using the chiral selector as bulk chiral ionic liquid rather than as additive in achiral ionic liquid, although such observations only refer to cases with bistriflimide anions, resulting in low melting points and therefore in room temperature CILs [20]. According to the present comparative experiments the chiral $[NopolMIm]^+$ selector looks more powerful when employed as DES component rather than as IL additive, with a dramatic modulation depending from the nature of the HBD component. In fact, the enantiomer peak potential difference remarkably increases in the order DES U<DES G<<<DES A, reaching an impressive ~0.5 V difference in the levulinic acid case. The enantiomer sequence is the same in all cases, as reasonable considering that the chiral selector is kept the same, *i.e.* $[NopolMIm]^+$.

The improved chiral selector performance of $[NopolMIm]^+$ as DES component respect to when used as IL additive in the DES cases could be at least partially (see above) justified with its higher concentration. However, the impressive difference in the three performances observed in the present case with the chiral selector at the same mole fraction in the three DESs, points to a fundamental role of the nature of the DES achiral partner, with the real huge improvement being observed in the case of DES A. The latter case, on account of the above considerations, could be considered a peculiar case, maybe even a task-specific chiral DES for amino compounds, hinging on specific acid/base interactions beyond general-scope interactions based on the available heteroatoms and aromatic rings.

Given the availability of a single enantiomer of the chiral selector [NopolMIm]Mes, corresponding to the configuration of its natural building block, we were unable in this case to perform our usual "double inversion" enantioselection check, consisting in verifying that a specular response is obtained inverting either probe or selector configuration. However, our chosen probe molecule, undergoing a reversible electrode process resulting in none or little electrode filming, enabled an even stronger verification experiment, *i.e.* racemate resolution.

In fact, as shown in Figure 6a, working in DES A with a 1:1 solution of (*R*)-Fc and (*S*)-Fc results in two neatly separated peaks, located at potentials close to the single enantiomer ones. Experiments carried out with mixed enantiomer solutions in different ratios, varying one enantiomer while keeping the other constant (Figures 6b and 6c), show a good dynamic range with concentrations and confirm that the two peaks correspond to the same enantiomers as in the single experiments, *i.e.* the (*S*) one at about -0.2 V preceding the (*R*) one at about 0.3 V. The first peak looks sharper and better reproducible/with a better dynamic range than the second one, which might be ascribed to the first process partially conditioning the interphase and affecting the result of the following one. Notably, although the peak separation looks narrower on C than on Au (SI 4), a large enantiomer resolution is obtained on all the SPE cells tested; this feature is also important, since it can be regarded as an indicator of the robustness of the proposed approach to enantioselective voltammetry based on chiral DES.

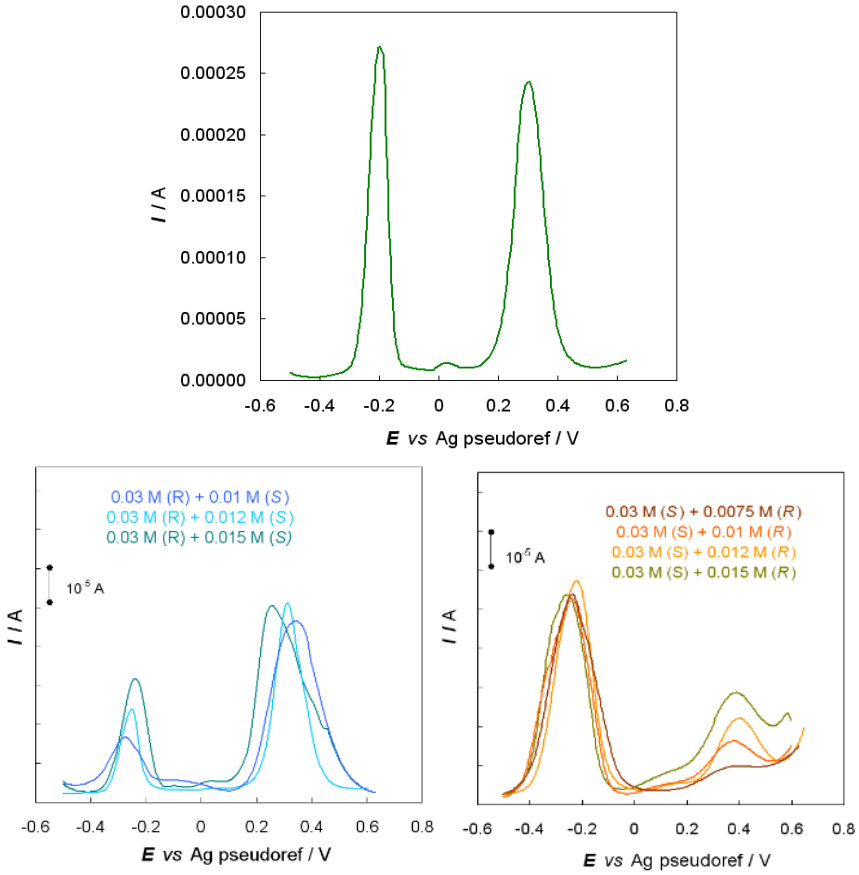

Figure 6. DPV patterns of (*R*)-Fc and (*S*)-Fc mixed solutions on Au SPE in DES A.

The enantiodiscrimination ability of DES A was also tested with the L- and D- antipodes of aminoacid tryptophan, an example of chiral probe of applicative interest, very different from the former one and undergoing a chemically irreversible first oxidation. Notably, it includes two N sites, both of which however have the N doublet by far less available than the tertiary amine one in the model Fc probes. In fact, in this case the amino group is involved in highly favoured zwitterion formation by intramolecular neutralization equilibrium with the carboxylic group; on the other hand, the doublet of the indolic N is involved in the conjugation of the heteroaromatic system, so that the indole basicity is very weak, and with protonation taking place in C_3 position rather than on the N atom [50,51], so two pK_as are usually reported for tryptophan, referred to COOH and NH_3^+ as in the simplest amino acid cases [52].

The tests were performed at different enantiomer concentrations, by DPV in a drop of DES A (with a small addition of aqueous KCl as in the former case) on C SPEs, *i.e.* on graphite working electrodes. For sake of comparison, the tryptophan antipodes were also tested with the same protocol in achiral BMIMTf$_2$N ionic liquid. The results are summarized in Figure 7.

Clear enantiodiscrimination is observed also in this case, with a peak potential difference of ~0.23 V for the two enantiomers in DES A (while the peak potentials are practically coincident in the achiral medium, Figure 7 top); a remarkable one, although not so outstanding as in the Fc case, which might be justified by the above comparison of N group availability. Moreover, also in this case a linear dynamic range with very good correlation coefficients is observed for peak currents as a function of concentration for both enantiomers (Figure 7 bottom).

This second experiment confirms that working in a suitable chiral DES large enantiomer peak potential differences can be obtained also with significantly different chiral probes, and with good linear dynamic ranges for peak currents. This combination provides a most desirable background for the development of effective protocols for qualitative and quantitative electroanalysis of chiral electroactive probes in chiral DESs.

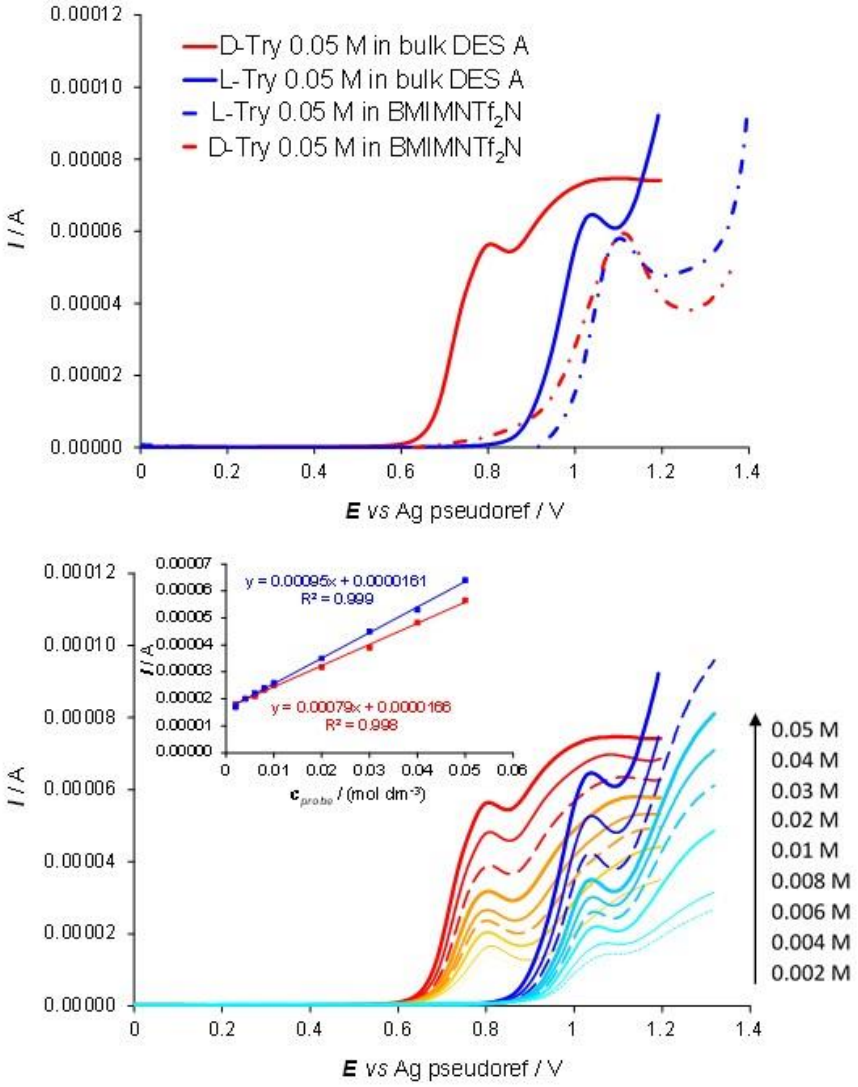

Figure 7. A synopsis of DPV features of D- and L- tryptophan (red and blue, respectively) in chiral DES A on C SPEs. Top: comparison with the same protocol in achiral $BMIMTf_2N$ at 0.05 M concentration. Bottom: verification of peak current vs concentration linearity for each enantiomer.

Conclusions

The results presented here constitute the first proof of concept of the remarkable potentialities of enantiopure chiral DESs as selector media for enantioselective electrochemistry and electroanalysis. DES interphases, although less defined and expanded than IL ones, and involving a higher amount of packing/clustering *vs* ion layering effects according to the first available studies [33-40], definitely look able to provide effective enantiodiscrimination in electron transfers involving chiral electroactive probes. Even more, the performances as chiral selector of our investigated molecular

salt with biobased cation appear enhanced when it is employed as DES component rather than as IL additive.

In the case of DES A, the results are particularly impressive, since a selector with stereocentre-based stereogenicity results in a striking outcome, similar to performances obtained with very powerful inherently chiral selectors. In particolar, large to huge DPV potential differences as well as good linear dynamic ranges for currents, a most desirable combination for development of quali/quantitative electroanalysis protocols, are obtained for the enantiomers of two quite different electroactive chiral probes, a model ferrocenyl amine one, and tryptophan, an amino acid of applicative interest.

Such proof-of-concept results also suggest many interesting developments, including a deeper investigation of the molecular interactions within the three-actor (probe and DES components) system, as such and at the interphase with the charged electrode surface, and a further analysis of the role of acid/base interactions. These studies should be regarded as an important step further in the frontier field of enantioselective electroanalysis and, more generally, can positively impact the development of task-specific enantioselective media and also promote development of DESs with more powerful stereogenicity elements in the chiral component.

Conflicts of interest

There are no conflicts to declare.

Acknowledgements

The paper is dedicated to Professor Cinzia Chiappe, Founder and Mentor of the Ionic Liquids Group at Pisa University.

Support of Fondazione Cariplo and Regione Lombardia (2016-0923 RST−Avviso congiunto FC-RL Sottomisura B) rafforzamento (Enhancing VINCE (Versatile INherently Chiral Electrochemistry)) are gratefully acknowledged, as well as advanced facilities available at SmartMatLab at Department of Chemistry, Università degli Studi di Milano, operated by Dr. Serena Cappelli.
Davide Grecchi is also acknowledged for the TOC photograph.

References

[1] A. Shishov, A. Bulatov, M. Locatelli, S. Carradori, V. Andruch, Application of deep eutectic solvents in analytical chemistry. A review, Microchem. J. 135 (2017) 33–38.
[2] Q. Zhang, K. De Oliveira Vigier, S. Royer, F. Jérôme, Deep eutectic solvents: syntheses, properties and applications, Chem. Soc. Rev. 41 (2012) 7108–7146.
[3] C. M. A. Brett, Deep eutectic solvents and applications in electrochemical sensing, Curr. Opin. Electrochem. 10 (2018) 143-148.
[4] B. Kudłak, K. Owczarek, J. Namieśnik, Selected issues related to the toxicity of ionic liquids and deep eutectic solvents—a review, Environ. Sci. Pollut. Res 22 (2015) 11975–11992.
[5] M. Espino, M. de los Ángeles Fernández, F. J.V. Gomez, M. Fernanda Silva, Natural designer solvents for greening analytical chemistry, Trends Anal. Chem. 76 (2016) 126–136.
[6] Y. Liu, J. Brent Friesen, J. B. McAlpine, D. C. Lankin, S. Chen, G. F. Pauli, Natural Deep Eutectic Solvents: Properties, Applications, and Perspectives, J. Nat. Prod. 81 (2018) 679-690.
[7] H. Vanda, Y. Dai, E. G. Wilson, R. Verpoorte, Y. H. Choi, Green solvents from ionic liquids and deep eutectic solvents to natural deep eutectic solvents, C. R. Chimie 21 (2018) 628-638.
[8] M. A. R. Martins, S. P. Pinho, J. A. P. Coutinho, Insights into the Nature of Eutectic and Deep Eutectic Mixtures, J. Solution Chem. 48 (2019) 962–982.
[9] S. Fryars, E. Limanton, F. Gauffre, L. Paquin, C. Lagrost, P. Hapiot, Diffusion of redox active molecules in deep eutectic solvents, J. Electroanal. Chem. 819 (2018) 214–219.
[10] F. Zhen, L. Percevault, L. Paquin, E. Limanton, C. Lagrost, P. Hapiot, Electron Transfer Kinetics in a Deep Eutectic Solvent, J. Phys. Chem. B 124 (2020) 1025−1032.
[11] S. Arnaboldi, M. Magni, P. Mussini, Enantioselective selectors for chiral electrochemistry and electroanalysis: Stereogenic elements and enantioselection performance, Curr. Opin. Electrochem. 8 (2018) 60-72.
[12] M. Z. Bazant, B.D. Storey, A.A. Kornishev, Double Layer in Ionic Liquids: Overscreening versus Crowding, Phys. Rev. Lett. 106 (2011) 046102/1-046102/4.
[13] S. Perkin, L. Crowhurst, H. Niedermeyer, T. Welton, A.A. Smith, N.N. Goswami, Self-assembly in the electrical double layer of ionic liquids, Chem. Commun. 47 (2011) 6572-6754.
[14] V. Ivaništšev, K. Kirchner, M.V. Fedorov, Restructuring of the electrical double layer in ionic liquids upon charging, J. Phys. Condens. Mater. 27 (2015) 102101/1-102101/5.
[15] V. Ivaništšev, S. O'Connor, M.V. Fedorov, Poly(a)morphic portrait of the electrical double layer in ionic liquids, Electrochem. Commun. 48 (2014) 61–64.
[16] K. Ma, R. Jarosova, G.M. Swain, G. J. Blanchard, Charge-Induced Long-Range Order in a Room-Temperature Ionic Liquid, Langmuir 32 (2016) 9507–9512.
[17] Y. Wang, R. Jarošová, G. M. Swain, G. J. Blanchard, Characterizing the Magnitude and Structure-Dependence of Free Charge Density Gradients in Room-Temperature Ionic Liquids, Langmuir 36 (2020) 3038-3045.

[18] T. Cui, A. Lahiri, T. Carstens, N. Borisenko, G. Pulletikurthi, C. Kuhl, F. Endres, Influence of Water on the Electrified Ionic Liquid/Solid Interface: A Direct Observation of the Transition from a Multilayered Structure to a Double-Layer Structure, J. Phys. Chem. C 120 (2016) 9341–9349.
[19] Y. Zhong, J. Yan, M. Li, L. Chen, B. Mao, The Electric Double Layer in an Ionic Liquid Incorporated with Water Molecules: Atomic Force Microscopy Force Curve Study, ChemElectroChem 3 (2016) 2221–2226.
[20] S. Rizzo, S. Arnaboldi, V. Mihali, R. Cirilli, A. Forni, A. Gennaro, A. A. Isse, M. Pierini, P. R. Mussini, F. Sannicolò, "Inherently chiral" Ionic-Liquid Media: Effective Chiral Electroanalysis on Achiral Electrodes, Angew. Chemie 56 (2017) 2079-2082.
[21] S. Rizzo, S. Arnaboldi, R. Cirilli, A. Gennaro, A. A. Isse, F. Sannicolò, P. R. Mussini, An "inherently chiral" 1,1'-bibenzimidazolium additive for enantioselective voltammetry in ionic liquid media, Electrochem. Comm. 89 (2018) 57-61.
[22] M. Longhi, S. Arnaboldi, E. Husanu, S. Grecchi, I. F. Buzzi, R. Cirilli, S. Rizzo, C. Chiappe, P. R. Mussini, L. Guazzelli, A family of chiral ionic liquids from the natural pool: Relationships between structure and functional properties and electrochemical enantiodiscrimination tests, Electrochim. Acta 298 (2019) 194–209.
[23] S. Grecchi, C. Ferdeghini, M. Longhi, A. Mezzetta, L. Guazzelli, S. Khawthong, F. Arduini, C. Chiappe, A. Iuliano, P. R. Mussini, Chiral biobased ionic liquids with cations or anions including bile acid building blocks as chiral selectors in voltammetry, ChemElectroChem, accepted March 2021.
[24] F. Fontana, G. Carminati, B. Bertolotti, P. R. Mussini, S. Arnaboldi, S. Grecchi, R. Cirilli, L. Micheli, S. Rizzo, Helicity: A Non-Conventional Stereogenic Element for Designing Inherently Chiral Ionic Liquids for Electrochemical Enantiodifferentiation, Molecules 26 (2021) 311-324.
[25] S. Arnaboldi, T. Benincori, A. Penoni, L. Vaghi, R. Cirilli, S. Abbate, G. Longhi, G. Mazzeo, S. Grecchi, M. Panigati, P. R. Mussini, Highly Enantioselective "Inherently Chiral" Electroactive Materials Based on the 2,2'-Biindole Atropisomeric Scaffold, Chem. Sci. 10 (2019) 2708-2717.
[26] N. Katsonis, E. Lacaze, A. Ferrarini, Controlling chirality with helix inversion in cholesteric liquids, J. Mater. Chem. 22 (2012) 7088-7097.
[27] S. Matsushita, B. Yan, S. Yamamoto, Y.S: Jeong, K. Akagi, Helical carbon and graphite films prepared from helical poly(3,4-ethylenedioxythiophene) films synthesized by electrochemical polymerization in chiral nematic liquid crystals, Angew. Chem. Int. Ed. 53 (2014) 1659–1663.
[28] B. Yan, S. Matsushita, K. Akagi, An advanced method for preparation of helical carbon and graphitic films using a carbonization substrate, Chem. Mater. 28 (2016) 8781–8791.
[29] S. Ahn, S. Yamakawa, K. Akagi, Liquid crystallinity-embodied imidazolium-based ionic liquids and their chiral mesophases induced by axidally chiral tetra-substitued binaphthyl derivatives, J. Mater. Chem. C 3 (2015) 3960-3970.
[30] S. Yamakawa, K. Wada, M. Hidaka, T.Hanasaki, K. Akagi, Chiral liquid-crystalline ionic liquid systems useful for electrochemiscal polymerization that affords helical conjugated polymers, Adv. Funct. Mater. 29 (2019) 1806592.
[31] L. VandeElzen, T. A. Hopkins, Monosaccharide-Based Deep Eutectic Solvents for Developing Circularly Polarized Luminescent Materials, ACS Sustain. Chem. Eng. 7 (2019) 16690-16697.
[32] T. Palomba, G. Ciancaleoni, T. Del Giacco, R. Germani, F. Ianni, M. Tiecco, Deep Eutectic Solvents formed by chiral components as chiral reaction media and studies of their structural properties, J. Molec. Liq. 262 (2018) 285-294.
[33] Z. Chen, B. McLean, M. Ludwig, R. Stefanovic, G.G. Warr, G.B. Webber, A. J. Page, R. Atkin, Nanostructure of Deep Eutectic Solvents at Graphite Electrode Interfaces as a Function of Potential, J. Phys. Chem. C 120 (2016) 2225−2233.
[34] M. Atilhan, S.Aparicio, Deep Eutectic Solvents on the Surface of Face Centered Cubic Metals, J. Phys. Chem. C 120 (2016) 10400−10409.

[35] S. Kaur, S. Sharma, H. K. Kashyap, Bulk and interfacial structures of reline deep eutectic solvent: A molecular dynamics study, J. Chem. Phys. 147 (2017) 194507-194510.
[36] Z. Chen, M. Ludwig, G.G. Warr, R. Atkin, , Effect of cation alkyl chain length on surface forces and physical properties in deep eutectic solvents, J. Colloid Interf. Sci. 494 (2017) 373–379.
[37] P. Sebastian, E. Gomez, V. Climent, J.M. Feliu, Investigating the M(hkl)| ionic liquid interface by using laser induced temperature jump technique, Electrochim. Acta 311 (2019) 30-40.
[38] K. Häckl, H. Li, I. M. Aldous, T. Tsui, W. Kunz, A. P. Abbott, G.G. Warr, R. Atkin, Potential Dependence of Surfactant Adsorption at the Graphite Electrode/Deep Eutectic Solvent Interface, J. Phys. Chem. Lett. 10 (2019) 5331−5337.
[39] O. S. Hammond, H. Li, C. Westermann, A.Y.M. Al-Murshedi, F. Endres, A. P.Abbott, G.G. Warr, K. J. Edler, R. Atkin, Nanostructure of the deep eutectic solvent/ platinum electrode interface as a function of potential and water content, Nanoscale Horiz. 4 (2019) 158-168.
[40] M. H. Mamme, S. L. C. Moors, E.A. Mernissi Cherigui, H. Terryn, J. Deconinck, J. Ustarroz, F. De Proft, Water distribution at the electrified interface of deep eutectic solvents, Nanoscale Adv. 1 (2019) 2847–2856.
[41] N. Zec, G. Mangiapia, M. L. Zheludkevich, S. Busch, J.-F. Moulin, Revealing the interfacial nanostructure of a deep eutectic solvent at a solid electrode, Phys.Chem.Chem.Phys. 22 (2020) 12104-12112.
[42] T. Zhekenov, N. Toksanbayev, Z. Kazakbayeva, D. Shah, F. S. Mjalli, Formation of type III Deep Eutectic Solvents and effect of water on their intermolecular interactions, Fluid Ph. Equilibria 441 (2017) 43-48.
[43] M. Francisco, A. van den Bruinhorst, M.C. Kroon, Low-Transition-Temperature Mixtures (LTTMs): A New Generation of Designer Solvents, Angew. Chem. Int. Ed. 52 (2013) 3074-3085.
[44] L.J.B.M. Kollau, M. Vis, A. van den Bruinhorst, G. de With, R. Tuinier, Activity modelling of the solid–liquid equilibrium of deep eutectic solvents, Pure Appl. Chem. 91 (2019) 1341–1349.
[45] D. O. Abranches, M. A. R. Martins, L. P. Silva, N. Schaeffer, S. P. Pinho, J. A. P. Coutinho, Phenolic hydrogen bond donors in the formation of non-ionic deep eutectic solvents: the quest for type V DES Chem. Commun. 55 (2019) 10253
[46] R. Craveiro, I. Aroso, V. Flammia T. Carvalho, M. T. Viciosa, M. Dionísio, S. Barreiros, R.L. Reis, Properties and thermal behavior of natural deep eutectic solvents, J. Mol. Liq. 215 (2016) 534–540.
[47] B.-A. Mei, O. Munteshari, J. Lau, B. Dunn, L. Pilon, Physical interpretations of Nyquist Plots for EDLC Electrodes and Devices, J. Phys. Chem. C 122 (2018) 194-206.
[48] K.W. Pratt, W. F. Koch, Y.C. Wu, P.A. Berezansky, Molality-based primary standards of electrolytic conductivity (IUPAC technical report) Pure Appl. Chem. 73 (2011) 1783-1793.
[49] I. M. Kolthoff, J. J. Lingane, Polarography, Vol. 1 (2nd Ed.), Interscience, New York, 1952, 189–234
[50] R. L. Hinman, E. B. Whipple, The protonation of indoles: position of protonation, J. Am. Chem. Soc. 84 (1962) 2534-2539.
[51] R. L. Hinman, J. Lang, The protonation of indoles: basicity studies. The dependence of acidity functions on indicator structure, J. Am. Chem. Soc. 86 (1964) 3796-3806.
[52] L. A. Kochergina, W. W. Chernikov, O. V. Platonykeva, Thermodynamics of stepwise dissociation of D-, L-tryptophan in aqueous solution, Russian J. Phys. Chem. A, 85 (2011) 938-943.